

Compositional analysis of thin $\text{SiO}_x\text{N}_y\text{:H}$ films by heavy-ion ERDA, standard RBS, EDX and AES: a comparison

W. Böhne ^{a,*}, J. Röhrich ^a, A. Schöpke ^a, B. Selle ^a, I. Sieber ^a, W. Fuhs ^a,
Á. del Prado ^b, E. San Andrés ^b, I. Mártel ^b, G. González-Díaz ^b

^a *Hahn-Meitner-Institut Berlin, Abt. Silizium-Photovoltaik, Kekuléstr. 5, D-12489 Berlin, und Ionenstrahl-Labor, Glienicke Str. 100, Berlin D-14109, Germany*

^b *Departamento de Física Aplicada III, Facultad de Ciencias Físicas, Universidad Complutense de Madrid, Madrid E-28040, Spain*

Received 21 August 2003; received in revised form 24 October 2003

Abstract

The composition of silicon oxynitride ($\text{SiO}_x\text{N}_y\text{:H}$) films deposited by electron cyclotron resonance chemical vapour deposition (ECR-CVD) was analysed by ion beam techniques, heavy-ion elastic recoil detection analysis (HI-ERDA) with 150 MeV ^{86}Kr ions and Rutherford backscattering spectroscopy (RBS) with 1.4 MeV ^4He ions. The results were compared with energy dispersive X-ray analysis (EDX) and Auger electron spectroscopy (AES). Since HI-ERDA provides absolute atomic concentrations of all film components including hydrogen with a sensitivity of at least 0.005 at% the data from this method were used as a quantitative reference to assess the applicability of RBS, EDX and AES to the analysis of silicon oxynitrides. For each of these techniques the comparison with HI-ERDA allowed a discussion of the different sources of error, especially of those causing systematic deviations of the measured concentration values. A novel approach to determine from RBS spectra also the hydrogen concentrations appeared to be applicable for hydrogen levels exceeding 2 at%. Furthermore, it is shown that the film density can be determined from the HI-ERDA results alone or in combination with single-wavelength ellipsometry.

© 2003 Elsevier B.V. All rights reserved.

PACS: 61.85; 82.80.P; 78.70.N; 61.50.N

Keywords: Elastic recoil detection analysis; Rutherford backscattering; Energy dispersive X-ray analysis; Auger electron spectroscopy; Silicon oxynitride; Electron cyclotron resonance plasma deposition; Thin film characterisation

1. Introduction

The desire to merge the most advantageous physical properties of both SiO_2 and Si_3N_4 in an

optimum combination tailored to various applications in electrical, optical and optoelectronic thin film devices has made silicon oxynitride (SiO_xN_y) thin films a subject of continuing scientific interest [1]. By controlling the composition of these films it is possible to optimally adjust quantities such as band gap, dielectric constant, stress, density and refractive index which are important for the performance of a device. A prominent

* Corresponding author. Tel.: +49-30-8062-2731; fax: +49-30-8062-2293.

E-mail address: bohne@hmi.de (W. Böhne).

example are gate insulators (and passivating layers) in Si metal-insulator-semiconductor (MIS) transistors where silicon oxynitride films seem to be more resistant against degradation and radiation damage than SiO_2 films. This is an important property with respect to long-term stability and space applications of these devices [2,3]. In order to optimise the film properties in the context of a specific device application, it is essential to control and to analyse the film composition as accurately as possible.

Recently, Walker et al. [4] have carried out a comparative composition analysis of silicon oxynitride films using the ion beam techniques heavy-ion energy recoil detection analysis (HI-ERDA) and nuclear reaction analysis (NRA). In the present paper, we report on a comparative compositional analysis of $\text{SiO}_x\text{N}_y\text{:H}$ films with four different methods based on X-ray, electron and ion scattering. In particular energy dispersive X-ray spectroscopy (EDX), Auger electron spectroscopy (AES), Rutherford backscattering spectroscopy (RBS) and HI-ERDA were used. These methods are different not only in their physical principle but also with respect to several practical aspects. For example, EDX and AES require calibration and, therefore, appropriate standards are necessary, whereas RBS and HI-ERDA provide quantitative composition data directly and can be used to quantify EDX and AES. Other relevant issues include background correction of the measured spectra and the modification of the film composition during the analysis, e.g. by particle beam induced ion-mixing or the release of volatile components, such as nitrogen and hydrogen. A comparison of results collected with different techniques for the same samples may be expected to give detailed information on the significance of such effects.

The films analysed in this study were grown by electron cyclotron resonance chemical vapour deposition (ECR-CVD) which is an advantageous technique to deposit oxynitride films at low substrate temperatures and to realise low-thermal budget concepts for device technology [5–7]. Since in this plasma-enhanced deposition process SiH_4 is used as a precursor gas, the incorporation of hydrogen is an inherent feature of the resulting

films and, thus, hydrogen detection is a special challenge to compositional analysis. It will be shown that HI-ERDA is the only of the four applied methods which is able to provide a complete composition analysis of $\text{SiO}_x\text{N}_y\text{:H}$ films including especially a reliable determination of the hydrogen concentration.

2. Experimental procedure

2.1. Sample preparation

The $\text{SiO}_x\text{N}_y\text{:H}$ films were grown simultaneously on high-resistivity silicon and on glassy carbon substrates by the ECR-CVD technique using an Astex plasma source (model AX4500). The film composition was controlled by carefully adjusting the flow rates of the precursor gases O_2 , N_2 and SiH_4 [8]. The total gas flow, the deposition pressure and the plasma power were kept constant at 10.52 sccm, 0.7 mTorr and 100 W, respectively. Two different series of samples were deposited with fixed flow ratios $R = (\text{O}_2 + \text{N}_2)/\text{SiH}_4$ of $R = 1.6$ and 5.0, respectively. For each series the fractional flow ratio $Q = \text{O}_2/\text{SiH}_4$ was varied which resulted in film compositions spanning the entire composition range between stoichiometric SiO_2 and Si_3N_4 . The as deposited samples were cut into square slices ($1 \times 1 \text{ cm}^2$) providing sets of identical history. The film thickness was determined for each sample by single-wavelength ellipsometry ($\lambda = 632.8 \text{ nm}$) and ranged from 250 to 450 nm.

2.2. Energy dispersive X-ray analysis

Energy dispersive X-ray spectra were recorded in a scanning electron microscope Hitachi S-4100 equipped with a field-emission cold cathode as an electron source and a $\text{Si}(\text{Li})$ X-ray detector of the type Pioneer Ultra Noran. A typical spectrum is shown in Fig. 1. Typically, the electron accelerating voltage was 5 kV and the detection take-off angle 30° . Films deposited on carbon substrates were investigated in order to ensure that the Si emission line was not influenced by contributions originating from the substrate. Stoichiometric films of SiO_2 and of Si_3N_4 from Noran served as

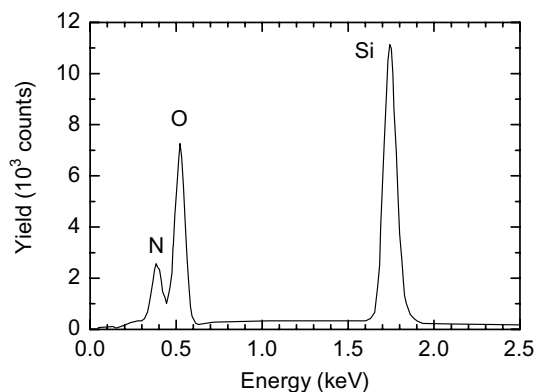


Fig. 1. The EDX spectrum of a typical $\text{SiO}_x\text{N}_y\text{:H}$ film with similar amounts of nitrogen and oxygen. Electron beam energy: 5 keV, take-off angle: 30° .

standards for the calculation of the film composition. The so-called PROZA correction [9] was applied to determine the relative atomic fractions of the three components N, O and Si. Hydrogen can not be detected by this method.

2.3. Auger electron spectroscopy

The AES measurements were performed with a cylindrical mirror analyser (PHI Mod. 10–155) with an energy resolution $\Delta E/E = 0.6\%$. The energy of the primary electrons was 5 keV. The Auger spectra were recorded in the derivative mode with a modulation of 4 eV_{ss}. In order to check the homogeneity of the film composition, depth profiling was carried out by alternating measurements of Auger spectra and sputtering the sample surface with 4 keV Ar^+ ions. A typical AES survey spectrum, which was recorded after several sputtering cycles, representing the composition within the film bulk, is shown in Fig. 2. The minimum-to-maximum intervals of the N, O and Si KLL lines were used in the analysis.

2.4. Rutherford backscattering spectrometry

The RBS spectra were measured with a 1.4 MeV $^4\text{He}^+$ ion beam of 1 mm diameter at the Tandatron accelerator JULIA of the University Jena. The detection angle was 170° , the beam current was ~ 20 nA and the accumulated charge at least 10 μC .

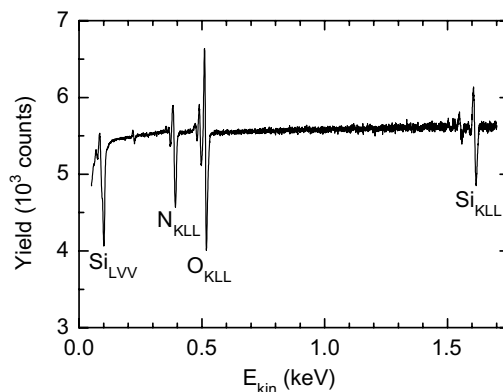


Fig. 2. First-derivative AES survey spectrum of a $\text{SiO}_x\text{N}_y\text{:H}$ film recorded after removing the near-surface part of the film by several sputter cycles.

After a background correction the spectra were analysed using the computer program RUBSODY [10], which performs iterative simulations to find a set of input parameters giving the best fit of the experimental data. This parameter set includes the element concentrations (except that of hydrogen) as well as the areal density $N \cdot d$ of the film where N is the atomic volume density and d is the film thickness. The background correction in the energy region of the oxygen and nitrogen signals turned out to be the most critical procedure in attaining correct results. A background-corrected RBS spectrum of a $\text{SiO}_x\text{N}_y\text{:H}$ film together with two different simulations is presented in Fig. 3. The well separated part of the spectrum at the highest energies represents backscattering from Si while the fractions of the spectrum corresponding to O and N overlap. Since the hydrogen atoms, which are also present in the film, have a smaller mass than the He projectiles they do not contribute to the backscattering signal. Therefore, a difference is found between the spectrum simulated using the accumulated charge (dotted upper curve) and the experimental data points. It will be shown in Section 3.2 that the hydrogen content can be estimated from this difference.

2.5. Heavy-ion energy recoil detection analysis

The HI-ERDA measurements were carried out with the mass and energy dispersive time-of-flight

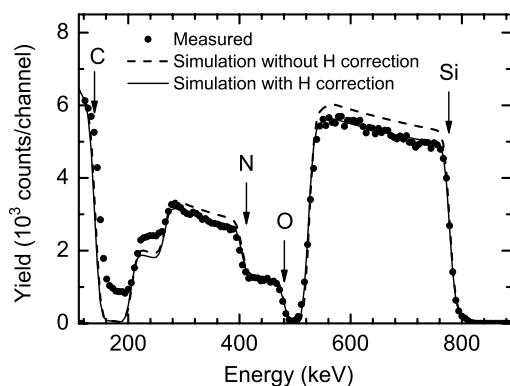


Fig. 3. Typical RBS spectrum of a $\text{SiO}_x\text{N}_y\text{:H}$ film recorded with $10 \mu\text{C } ^4\text{He}^+$ ions at 1.4 MeV. The upper dotted line is a simulation fit without taking into account the hydrogen content of the film, the solid line is a corrected fit (see text).

(TOF) set-up at the heavy-ion accelerator facility (ISL) of the Hahn-Meitner-Institut Berlin [11]. 150 MeV ^{86}Kr ions were employed as projectiles. The number of the incident particles was measured with an accuracy of $\pm 2\%$ using a “transmission Faraday cup” [12]. The detection system with a solid angle of 0.4 msr and the use of a large detection angle of 60° with respect to the beam direction provided acceptable statistics even for an ion fluence as low as 10^{12} cm^{-2} . As the scattering data were stored event by event, a sequential data evaluation for progressing measuring time, i.e. for increasing ion fluence, could be made. Ion-induced changes of the film composition were caused by losses of the “critical” elements H and N taking place under beam exposure. A non-linear correction procedure [13] was applied to correct these effects and to calculate the zero-dose composition of the films. The amount of depleted hydrogen and nitrogen during the ERDA measurements is very different depending on the composition of the samples. For films with a stoichiometry close to silicon oxide or silicon nitride the losses were only a few percent. For compositions between these extreme values we found, especially in the case of hydrogen, a reduction of up to almost 50%. The additional uncertainties due to this extrapolation are included in the error-bars in the corresponding figures.

Fig. 4 displays a representative scatterplot of time-of-flight (t_0 -TOF) versus energy E for a $\text{SiO}_x\text{N}_y\text{:H}$ film of medium-range composition, i.e. a sample with similar amount of nitrogen and oxygen on a Si substrate. The most intriguing plot feature is the band associated with recoiling Si atoms, which is dominated by the strong contribution of the substrate at lower energies, whereas the recoils of O, N and H originate exclusively from the deposited film and, therefore, form smaller sections of their relevant branches. The mass identified bands were transformed into energy spectra using the corresponding time-of-flight, because the time resolution is, especially for heavier elements, better than the energy resolution. This gives a better depth resolution. Furthermore, pulse-amplitude deficits due to ionisation defects in the Si-detector are avoided. To obtain the elemental concentrations in units of an areal density (atoms/ cm^2) all spectra were simultaneously fitted using the simulation code SIMNRA [14]. The computer program uses the stopping power parameter SRIM95 [15]. Note the small background level which allows the concentration measurement of all film components including hydrogen with fairly high sensitivity (below 0.005 at%).

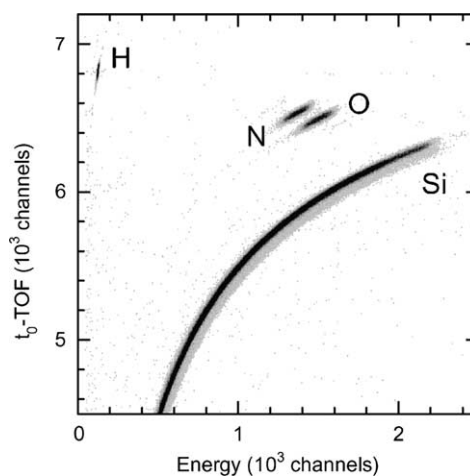


Fig. 4. Scatterplot (t_0 -TOF) versus energy of a $\text{SiO}_x\text{N}_y\text{:H}$ film ($x = 0.75$, $y = 0.94$, thickness $d = 250 \text{ nm}$) on Si measured with 150 MeV ^{86}Kr primary ions at a fluence of $1.1 \times 10^{14} \text{ cm}^{-2}$ (scattering angle: 60°).

3. Results and discussion

3.1. Comparison of the analysing methods

To compare the different techniques, Fig. 5 presents a joint plot of $x = [\text{O}]/[\text{Si}]$ versus $y = [\text{N}]/[\text{Si}]$ as calculated from the data obtained by HI-ERDA, RBS and EDX. The data points refer to the sample series deposited with $R = 1.6$ where, after previous experience with $\text{SiN}_x\text{:H}$ films [16], compositions close to a stoichiometric ratio of N, O and Si should be expected. In that case, the correlation between x and y is given by the electronic co-ordination numbers of N, O and Si and should satisfy the relation

$$2x + 3y = 4. \quad (1)$$

In Fig. 5 this relationship is represented by the solid line. It can be seen that this line is best approached by the HI-ERDA results while the RBS and EDX data reveal larger deviations, indicating an excess of the non-silicon components. For RBS this can be understood by the fact that the signal heights of N and O are more affected by an inaccurate background correction than the Si signal. Moreover, the simulation code does not include multiple scattering processes which contribute more at lower backscattering energies and, hence, are misinterpreted as a higher N or O concentration, respectively.

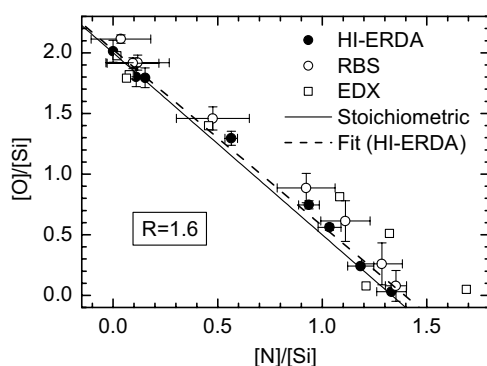


Fig. 5. Correlation between $x = [\text{O}]/[\text{Si}]$ and $y = [\text{N}]/[\text{Si}]$ in $\text{SiO}_x\text{N}_y\text{:H}$ films grown at a flow ratio $R = (\text{O}_2 + \text{N}_2)/\text{SiH}_4$ of 1.6. The HI-ERDA results (solid circles) are compared with RBS and EDX data (open symbols). The solid line represents stoichiometric composition according to Eq. (1), the dotted line is a linear fit to the HI-ERDA results.

In the case of EDX, a serious problem arises by the overlap of the N and O emission lines. A proper selection of the “regions of interest” and the choice of the optimum fit algorithm (Gaussian deconvolution or filter-fit method) influences the results, especially if one of the lines is of low intensity and produces only a weak shoulder in the line foot region of its high-intensity neighbour. In this case the Gaussian deconvolution was superior to the filter-fit method. Furthermore, since EDX does not provide any depth information, any native Si oxide formed at the sample surface leads to an enhanced O line intensity shifting the calculated oxygen concentrations to systematically higher values. This seems to be the main reason for the larger deviations of the EDX data in the lower right part of Fig. 5.

Since both overlap and background correction problems are not relevant for HI-ERDA and absolute concentrations of all film components, i.e. also of hydrogen, are detected, we conclude that HI-ERDA provides the most reliable composition analysis of $\text{SiO}_x\text{N}_y\text{:H}$ films compared to RBS and EDX. Therefore, the results obtained with this method can serve as a standard data base and are well suited to calibrate other non-standard-free analytical techniques.

Figs. 6(a) and (b) present more detailed examples to illustrate how the EDX results compare with the data set determined by HI-ERDA. While a good linear correlation is found for the $[\text{O}]/([\text{O}] + [\text{N}])$ ratio (Fig. 6(a)) the $([\text{O}] + [\text{N}])/[\text{Si}]$ ratio shows larger deviations from the linearity, especially in the intermediate composition range (Fig. 6(b)). Besides of the above mentioned sources of error, this behaviour is mainly due to the fact that the measured X-ray line intensities were quantified by reference samples of stoichiometric SiO_2 and Si_3N_4 . Obviously, this is not sufficiently adequate to provide an accurate evaluation over the entire composition range, but allows only an appropriate determination of film compositions close to pure Si oxide or nitride. For practical purposes it seems to be useful to complete the stock of EDX standards also by one or several films of intermediate composition which can be certified by HI-ERDA before.

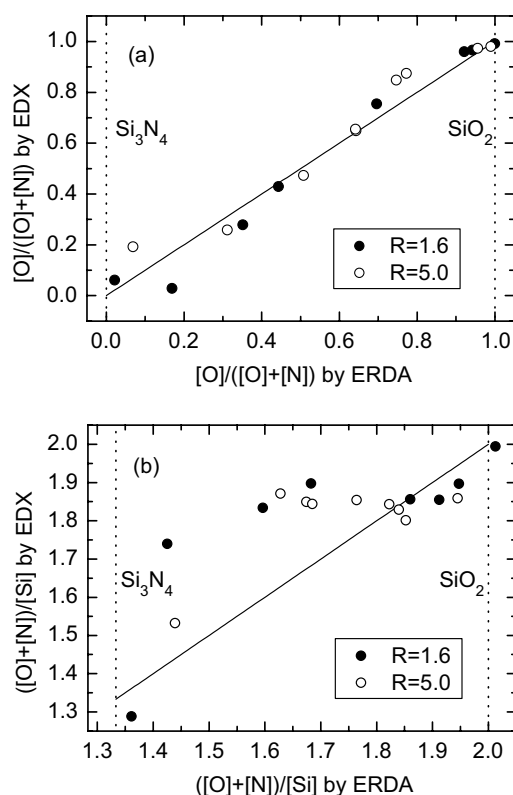


Fig. 6. Cross-check of the EDX and the HI-ERDA results for both sample series (solid symbols: $R = 1.6$, open symbols: $R = 5.0$): (a) ratio $[O]/([O] + [N])$, (b) ratio $([O] + [N])/[Si]$.

Finally, Fig. 7 shows a plot of the AES line intensity ratio $\{I(O_{KLL}) + I(N_{KLL})\}/I(Si_{KLL})$ as a function of the relevant concentration ratio $([O] + [N])/[Si]$ determined by HI-ERDA. Although one should expect some changes of the sensitivity factors due to the well known “matrix effect”, the AES line intensity ratio reveals a clear linearity with respect to the concentration ratio $[O + N]/[Si]$ derived from HI-ERDA. This means that, surprisingly, the relevant Auger sensitivity factors of the KLL lines of Si, O and N scale in a nearly identical way with the variation of the nitrogen, oxygen and, in particular, the hydrogen concentrations in the film. Thus, Fig. 7 presents a useful base for a straightforward calibration of the AES method by HI-ERDA reference data. The line slope in Fig. 7 might depend on the special experimental conditions of AES. Therefore, the

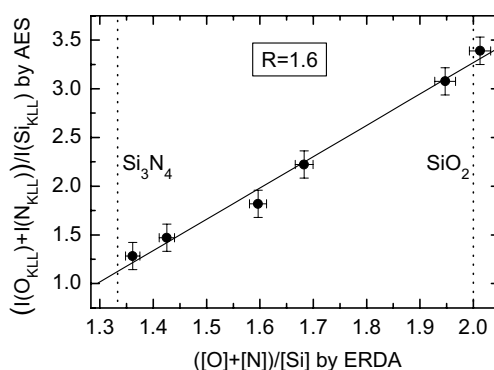


Fig. 7. AES line intensity ratio $\{I(O_{KLL}) + I(N_{KLL})\}/I(Si_{KLL})$ as a function of the relevant concentration ratio $([O] + [N])/[Si]$ determined by HI-ERDA for the sample series grown at $R = 1.6$. The line is a linear fit to the data.

calibration has to be performed for the experimental configuration which will be chosen for a quantitative analysis of silicon oxynitride films.

3.2. Hydrogen analysis

From the HI-ERDA data points of Fig. 5 a fit line can be calculated by linear regression which is not identical with the stoichiometry line resulting from Eq. (1). The small discrepancy may be caused by the presence of hydrogen in the films which to a first approximation was neglected in Eq. (1). As shown in Fig. 8 the hydrogen concentration in the studied $SiO_xN_y:H$ films increases linearly with the N concentration up to values of about 15 at% in the composition range approaching silicon nitride (line slope: 0.27 ± 0.02). Detailed studies of the bonding structure by IR phonon spectroscopy revealed that in these films hydrogen predominantly is bonded in a N–H configuration [17,18]. Thus, it is reasonable to modify in Eq. (1) the factor 3 which represents the co-ordination number of nitrogen in the following way:

$$2x + (3 - X_{NH})y = 4, \quad (2)$$

with X_{NH} as a measure for the intensity of the N–H configuration.

With this relationship a more exact description of the HI-ERDA results in Fig. 5 can be achieved [18]. However, the obtained fit value of $X_{NH} = 0.21 \pm 0.04$ is significantly lower than the

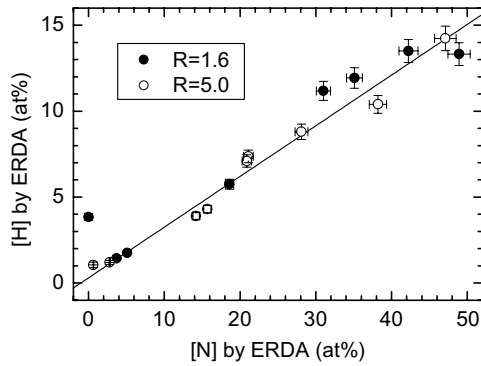


Fig. 8. Total hydrogen concentration determined by HI-ERDA as a function of the total nitrogen concentration. Solid symbols: $R = 1.6$, open symbols: $R = 5.0$. The solid line is a linear fit yielding a slope of 0.27 ± 0.02 .

line slope value of Fig. 8. This indicates that the model of Eq. (2) still does not adequately describe the complex network structure of a hydrogen-containing silicon oxynitride. Also, it does not take into account the amount of non-bonded hydrogen which might be present in the films.

Because the equipment for performing HI-ERDA is not easily accessible we have made an attempt to estimate the hydrogen concentration also from the standard RBS spectra. As already mentioned in Section 2.4 the hydrogen in the films does not contribute to the He ion backscattering and, thus, hydrogen was not included in the element list for the simulation procedure. This leads to a difference between the measured and the simulated yield (see Fig. 3) which increases with the hydrogen concentration in the film. From this signal difference the hydrogen concentration can be obtained, in turn, to a first approximation. Further improvements are possible if the stopping cross sections are modified taking into account the presence of hydrogen. This was attempted by inserting a low Z element (e.g. Be instead of H due to the restriction of the code used) as a substitute for hydrogen into the element list. Finally, a corrected simulation curve of the experimental data can be calculated (solid line in Fig. 3), again using the measured fluence. In Fig. 9 the hydrogen concentrations estimated from RBS spectra by this procedure are plotted against the HI-ERDA values. The error bars, which were obtained from the

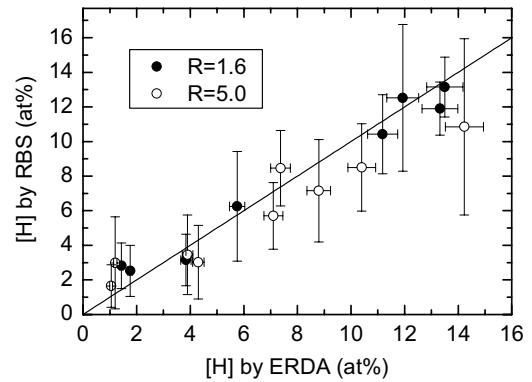


Fig. 9. Hydrogen concentration estimated from RBS spectra as a function of the hydrogen concentration measured by HI-ERDA. Solid symbols: $R = 1.6$, open symbols: $R = 5.0$. The line corresponds to a coincidence of the data.

results of repeated and slightly modified calculation cycles, are comparatively large. Although the coincidence line is well embedded within the error ranges it becomes evident that RBS can only provide a crude estimate of the hydrogen concentration that should be regarded with highest caution for values below 2 at%.

3.3. Film density

The determination of the film density is a problem of high practical relevance. Our HI-ERDA results allow to calculate this quantity in two ways. In the first approach the $\text{SiO}_x\text{N}_y\text{H}$ film is thought to be composed by a mixture of compact Si, SiO_2 and Si_3N_4 , with the corresponding mole fractions A , B and C ($A + B + C = 1$) and the low-mass hydrogen dissolved homogeneously within this mixture. A , B and C can be calculated from the measured concentrations of Si, O and N. The film density ρ_{film} is approximated by the expression

$$\rho_{\text{film}} = (1 - X_{\text{H}}) \cdot (A \cdot \rho_{\text{Si}} + B \cdot \rho_{\text{SiO}_2} + C \cdot \rho_{\text{Si}_3\text{N}_4}), \quad (3)$$

where X_{H} is the atomic fraction of hydrogen as measured by HI-ERDA. For ρ_{Si} , ρ_{SiO_2} and $\rho_{\text{Si}_3\text{N}_4}$ the corresponding bulk densities of these materials [19] were inserted.

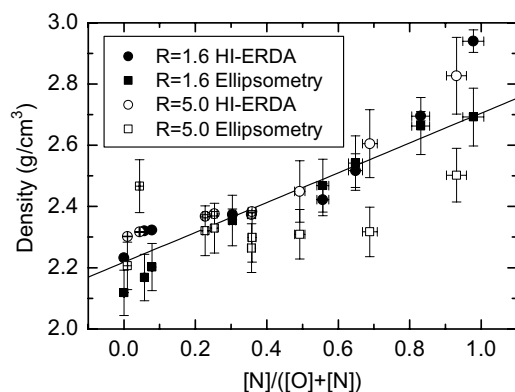


Fig. 10. Gravimetric density of the $\text{SiO}_x\text{N}_y\text{:H}$ films as a function of the ratio $[\text{N}]/([\text{O}] + [\text{N}])$ determined by HI-ERDA. Solid symbols: $R = 1.6$, open symbols: $R = 5.0$. Circles indicate results calculated by Eq. (3), squares are data obtained when dividing $N \cdot d$ by the ellipsometric thickness. The line represents a linear fit to all data.

In the second approach the areal density $N \cdot d$ of the films obtained by ERDA (or RBS) is combined with the film thickness measured by single-wavelength ellipsometry ($\lambda = 632.8 \text{ nm}$) [18] and the resulting atomic density N is transformed into a weight density. As shown in Fig. 10 the data of both approaches agree well within their error ranges and indicate an approximately linear increase of the density with the relative nitrogen content of the films. The ellipsometric densities appear to be generally smaller than the densities obtained from HI-ERDA, in particular for the films grown at $R = 5.0$. This might again be due to some fraction of non-bonded H, which does not form optically active oscillators, with the consequence that the ellipsometric measurement yields a systematically lower refractive index and a higher thickness which, finally, leads to a lower calculated atomic density.

4. Conclusions

A series of $\text{SiO}_x\text{N}_y\text{:H}$ films deposited by ECR-CVD have been studied in a comparative composition analysis carried out by high-energy HI-ERDA, standard RBS, EDX and AES. With a detection sensitivity as low as 0.005 at% for all film

components including also hydrogen, HI-ERDA turned out to provide the most accurate composition data in a single measurement. Since the method is absolute and does not need any calibration the obtained concentration values can be used as standard data sets to quantify other techniques. This feature was used to evaluate the analytical power of RBS, EDX and AES. In addition, HI-ERDA is the only one of these methods which is suitable to determine the total concentration of hydrogen in silicon oxynitride films, including the bonded and the non-bonded fractions. An attempt to estimate the hydrogen concentration from RBS spectra has revealed large error ranges of about $\pm 2 \text{ at\%}$ and might be useful only for films containing comparatively high levels of hydrogen. Although EDX does not deliver information on hydrogen, the other components (Si, O, N) can be readily analysed with sufficient accuracy if well certified reference samples are also available for the intermediate composition ranges. For the composition analysis by AES the problem of the matrix dependence of the sensitivity factors can be circumvented if not directly the line intensities but rather their ratios are considered. In spite of having certain weaknesses EDX, AES and standard RBS, nevertheless, are much more easily accessible than HI-ERDA and, if previously quantified by HI-ERDA, should be preferred in cases of an extended routine analysis involving larger sample quantities.

Acknowledgements

This study was supported in part by the German *Bundesministerium für Wirtschaft* (contract 0329773) and by the CICYT of Spain (contract TIC 01-1253).

References

- [1] Y. Ma, G. Lucovsky, J. Vac. Sci. Technol. B 12 (1994) 2504.
- [2] G.J. Dunn, R. Jayaraman, W. Yang, C.G. Sodini, Appl. Phys. Lett. 52 (1988) 1713.
- [3] G.Q. Lo, D.K. Shih, W.C. Ting, D.L. Kwong, Appl. Phys. Lett. 55 (1989) 840.

- [4] S.R. Walker, J.A. Davies, P. Mascher, S.G. Wallace, W.N. Lennard, G.R. Massoumi, R.G. Elliman, T.R. Ophel, H. Timmers, Nucl. Instr. and Meth. B 170 (2000) 461.
- [5] P.K. Shufflebotham, D.J. Thomson, H.C. Card, J. Appl. Phys. 64 (1988) 4398.
- [6] A. Popov, J. Vac. Sci. Technol. A 7 (1989) 894.
- [7] S. García, J.M. Martín, M. Fernández, I. Mártil, G. González-Díaz, Philos. Mag. B 73 (1996) 487.
- [8] A. del Prado, I. Mártil, M. Fernández, G. González-Díaz, Thin Solid Films 343–344 (1999) 437.
- [9] G.F. Bastin, H.J.M. Heijligers, Scanning 12 (1990) 225.
- [10] A. Witzmann, RUBSODY Users Guide, Friedrich-Schiller-Universität Jena, Institut für Festkörperphysik, 1992.
- [11] W. Böhne, J. Röhrich, G. Röschert, Nucl. Instr. and Meth. B 136–138 (1998) 633.
- [12] W. Böhne, S. Hessler, G. Röschert, Nucl. Instr. and Meth. B 113 (1996) 78.
- [13] W. Böhne, W. Fuhs, J. Röhrich, B. Selle, I. Sieber, A. del Prado, E. San Andrés, I. Mártil, G. González-Díaz, Surf. Interface Anal. 34 (2002) 749.
- [14] M. Mayer, SIMNRA Users Guide, Report IPP 9/113, Max-Planck-Institut für Plasmaphysik, Garching, 1997.
- [15] J.F. Ziegler, J.P. Biersack, U. Littmark, Stopping and Ranges of Ions in Solids, Pergamon, New York, 1985 and updates in the web site <http://www.srim.org/>.
- [16] F.L. Martínez, I. Mártil, G. González-Díaz, B. Selle, I. Sieber, J. Non-Cryst. Solids 227–230 (1998) 523.
- [17] L.-N. He, T. Inokuma, S. Hasegawa, Jpn. J. Appl. Phys. 35 (1996) 1503.
- [18] A. del Prado, E. San Andrés, F.L. Martínez, I. Mártil, G. González-Díaz, W. Böhne, J. Röhrich, B. Selle, M. Fernández, Vacuum 67 (2002) 507.
- [19] R.C. Weast, M.J. Astle, W.H. Beyer (Eds.), CRC Handbook of Chemistry and Physics, CRC Press, Boca Raton, 1987.